Design Space Method for Conceptual Design Exploration of High Speed Slitted Solid Induction Motor

Kurvinen Emil, Choudhury Tuhin, Narsakka Juuso, Martikainen Iikka, Sopanen Jussi, Jastrzebski Rafal

DOI: 10.1109/IEMDC47953.2021.9449526

Design Space Method for Conceptual Design Exploration of High Speed Slitted Solid Induction Motor

Emil Kurvinen, Tuhin Choudhury, Juuso Narsakka, Iikka Martikainen, Jussi Sopanen
Department of Mechanical Engineering
LUT School of Energy Systems
Lappeenranta-Lahti University of Technology LUT
Lappeenranta, Finland
emil.kurvinen@lut.fi, tuhin.choudhury@lut.fi, juuso.narsakka@lut.fi, iikka.martikainen@lut.fi, jussi.sopanen@lut.fi

Rafal P. Jastrzebski
Department of Electrical Engineering
LUT School of Energy Systems
Lappeenranta-Lahti University of Technology LUT
Lappeenranta, Finland
rafal.jastrzebski@lut.fi

***Abstract*—Design of High Speed (HS) electric machines is an iterative process that requires a multidisciplinary design team to accomplish the required performance. In this study, a design space method (DSM) is developed to streamline conceptual designing of a high-speed and high-power electric machine. The method uses analytical equations and a rotordynamic model to determine geometrical dimensions based on the application requirements. These dimensions create a feasible baseline design for the particular application. However, considering the dimensions as design variables and using the baseline design as a starting point, a multidimensional combination and interaction of the design variables and the correlated output for the particular topology of motor and performance range can be further studied for design exploration and optimization purposes. The study includes a test case where the baseline dimensions are determined and compared to an existing machine from literature, and then further explored to identify the sensitivity of different outputs with respect to different design variables. The method enables rapid design iterations, rotordynamics and rotor mass optimization. The baseline design can be also used as a starting point for the detailed design.**

***Index Terms*—Iterative Design, Design Space, High-speed, Electric Machines, Induction motor**

I. Introduction

High-Speed (HS) rotating machines can be categorized as special types of electric machines where the peripheral speed of the electric motor (EM) exceeds 100 m/s [1]. HS machines are often used as an integrated motor or generator in drive systems in applications such as compressors, blowers, flywheel energy storage and turbines [2]. Such machines are in high demand because of their high efficiency, small footprint, and the fact that they can facilitate a direct drive system, eliminating the use of gear systems and accessories [3].

Correlated recent trends show that such HS machines are preferably operated in combination with oil free bearing systems, leading to ordinary ball bearings, or fluid film bearings being replaced by Active Magnetic Bearings (AMB) [4], [5]. An AMB levitated rotor is free of contact friction, which reduces component wear and the requirement for frequent maintenance. Other benefits include reduced losses due to no contact friction, health monitoring, and lower vibration and noise [6].

The challenges in HS machines arise from the design and manufacturing perspective, especially in high-power machines as the quality requirements of the components are high and the machines are typically operating near their physical limits. The surface velocity or the peripheral speed of the electric machine, which is used to distinguish HS machines, is also one indicator of the design difficulty level. The higher the surface velocity, the more compact the machine is, but the more challenging aspect is to maintain the structural integrity of the rotor due to higher stresses. In addition, the EM topology used has an influence on the attainable surface velocities, i.e. solid rotors can have higher surface velocity than laminated structures [7]. The surface velocity can also be used as a design boundary condition, as it indicates the needed material strengths, quality and also manufacturing difficulty, see e.g. [8].

Over the years, many studies have proposed methodologies for design and manufacturing of permanent magnet and induction HS machines. [9]–[15]. High-power and HS machines and their designs are a strict compromise that attempts an optimal balance of electrical, thermal, application (impeller) and mechanical (design and manufacturing) disciplines [9]. This implies that the design changes (e.g. impeller, EM or bearing changes) lead to a full revision of the design to find the optimal combination of sub solutions. This, in turn, limits wider usage of the HS machines. Industrial trends are going especially for higher power machines and these require entirely new design, since the constructions typically used in smaller power machines cannot be extended to higher power ratings due to limits of rotordynamics factors.

The study utilizes the concept of design space (DS) where

the correlation between design variables (such as geometrical dimensions and impeller mass) and the performance related objective parameters of the motor (such as rotor mass, torque, critical speeds, etc.) can be used to create a design table for detailed analysis. The method uses analytical equations and a rotordynamic model to determine geometrical dimensions based on the application requirements. Using these dimensions of the 'baseline design' as a starting point, different combinations of dimensions (design variables) for different rotor sections and their effect on the motor performance and rotordynamics can be calculated to form the design table or 'design space' with different design alternatives in arrays. For example, a short electric machine yields good dynamical performance, however, cooling becomes demanding as the losses in the EM are generated in a short section. The novelty of the proposed method is that it allows rapid design iterations as the geometry configurations can be pre-calculated while the basic limits from electromagnetic, mechanical stress and rotordynamics are accounted for. This allows for more focus on the detailed electromagnetic and thermal design iterations, as the selection of specific EM tangential stress, which is also related to the cooling method, and AMB's specific load capacity guarantees the space to generate required torque and suspension force during the anticipated operation. This also enables iteration through the feasible design ranges. In addition, the nodal locations of the critical speeds can be included in the design, which are useful for the control design. The critical speed nodal locations affect the controllability of the modes, and the further away they are, the more controllability the modes can have [6]. Eventually, the process enables the observation of the different design configurations more objectively, when compared to traditional HS iterative design procedure, e.g. [9].

II. Mechanical Design for high speed (HS) induction machines with slitted rotor

A. Design process of High-Speed Electric Machine

Fig. 1 depicts a typical part in iterative high power HS EM design process, where mechanical design is performed in parallel with other design steps (left) and iterative design process with Design Space method (DSM) concept (right). In DSM, mechanical design boundary conditions are pre-calculated in the conceptual design phase and with the other factors i.e., the physical limitations (electromagnetic, thermal and structural limitions) are accounted for by analytical equations. These include tangential stress in the electric machine rotor surface, it can be used to assess the feasibility of the design from electrical and thermal perspectives [16]. Finally, the structural integrity can be assessed using analytical methods for the stresses generated by the centrifugal forces on the rotor and rotordynamics performance can be assessed with efficient and effective calculation methods such as linear Finite Element Method (FEM), used in mechanical design, allowing the possibility to study the design as a whole.

HS EM design is an iterative process and during the design process, iterations between different design disciplines (see Fig. 1) are performed [9]. Due to this, the design of the

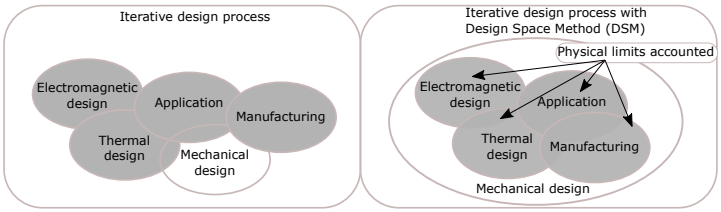

Fig. 1. Iterative design process without design space and with design space method

machines is time consuming and is typically counted in months. When considering the manufactured HS machines, the materials used are limited to a few materials due to the high requirements for manufacturing, tolerances and quality [10]. The machines typically operate near their physical limits and thus high-quality materials are needed to guarantee safe operation. The mechanical part of the design includes the structural and dynamical analyses of the rotating structure. In the design the geometry of the rotating structure and support structure are of interest, especially in high-power applications. Rotation speed of the rotor is typically limited by the dynamical performance, i.e., the first flexible bending mode of the supported rotor gets excited by the residual unbalance of the structure and leads to an excessive amount of vibration. In the analyses the Finite Element (FE) method is utilized. Computationally efficient beam element models are widely utilized in the conceptual design phase, since they can predict the dynamical behavior of cylindrical structures accurately [17]. Small computational time for single configuration enables the analysis of thousands of configurations within hours. Whereas, when making a comparison between electromagnetic or thermal analyses, the computational time for a single configuration takes substantially longer, as the number of equations that need to be solved is higher.

B. Design Space method for AMB supported HS machines

The Design Space method (DSM) is a systematic method for analyzing HS machine design with incremental and radical changes, while accounting for the physical limits. The overall objective is set by the requirements of the desired HS machine, e.g., required speed, power and dynamical behavior are used as inputs to the calculation tool [9].

The method divides the geometry into varied parameters which are changeable, e.g., the length of bearing or electric machine, and permanent parameters that are kept fixed, e.g., distance of sensor planes. By studying existing machines, physical limitations of design can be found, by e.g., by comparing the surface velocities of the proposed designs [18]. The physical limitations can be used as boundary conditions for detailed design. These are, for example, electric machine tangential stress for specified cooling solutions in different electric machine topology values [16] and AMB load capacity per area, ranging in a typical case of between 200 to 400 kN/m^2 (kPa) depending on the materials used [19], [20]. In addition, the structural integrity can be estimated by means of

analytical equations [21]. The varied dimension of the rotor are iterated according to structural boundary conditions and integration constraints (e.g. AMB stators located under the end winding of the electrical machine, integration of axial AMB). Considering these boundary conditions in structural analysis and rotordynamics, a baseline design can be created.

C. Baseline design dimensions from requirements

The geometrical dimensions of interests are the length and diameter of the active part of the rotor (l_{em}, d_{em}), the bearing sections (l_{amb}, d_{amb}), rotor ends (l_{end}, d_{end}), and other general sections (l_{sn}, d_{sn}) respectively. Fig. 2 shows the structure of a typical HS rotor with slitted rotor design.

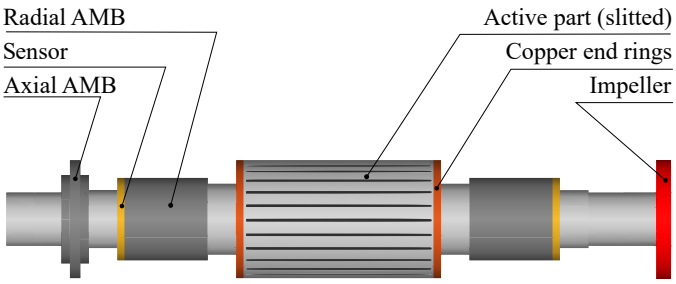

Fig. 2. A general model of a slitted rotor HS machine

The required power and the surface velocity are the defining factors for the dimensions of the active part of the rotor. Based on the material, the maximum mechanical stress can be approximated using the tensile stress and a stress concentration factor. For example, for a slitted rotor, where the highest stress due to the centrifugal force occurs at the root of the tooth, the nominal stress σ_{tooth} due to centrifugal force F_{c} acting at the tooth center of mass (r_{com}). Knowing the area of the tooth root ($A_{\text{r}} = w \cdot L$), where w is the width of the tooth root and L is the length of the tooth resulting [22] in

$$\sigma_{\text{tooth}} = \frac{F_{\text{c}}}{w \cdot L} = \frac{\rho \cdot A \cdot L \cdot r_{\text{com}} \cdot \omega^2}{w \cdot L} = \frac{\rho \cdot A \cdot r_{\text{com}} \cdot \omega^2}{w} \quad (1)$$

where ρ is mass density, A is the area of teeth, r_{cg} is the distance of tooth mass center from the axis of rotation and ω is the rotation speed. The maximum stress σ_{max} can be attained by multiplying the nominal stress by the stress concentration factor k_{tooth} resulting in $\sigma_{\text{max}} = k_{\text{tooth}} \cdot \sigma_{\text{tooth}}$, where the stress concentration factor can be estimated from [22].

To achieve high efficiency and minimize the rotor losses the copper end rings enhance the performance. For a hollow copper disk the stresses σ_{holdisk} can be calculated with

$$\sigma_{\text{holdisk}} = 1/4 \cdot \rho_{\text{d}} \cdot \omega^2 \cdot ((1 - \nu_{\text{d}}) \cdot r_{\text{in}}^2 + (3 + \nu_{\text{d}}) \cdot r_{\text{out}}^2), \quad (2)$$

where ν_{d} is the Poisson's ratio, ρ_{d} is the density of the disk, r_{in} is the disk inner radius and r_{out} outer radius [23].

The obtained value should also be verified for attainable surface velocity as

$$v_{\text{surf}} = \pi \cdot d_{\text{em}} \cdot \omega \quad (3)$$

Electric machines produce torque, and in the application the desired torque is typically known. The required electromagnetic tangential stress, σ_{Ftan}, in the electric machine rotor surface can be estimated as

$$\sigma_{\text{Ftan}} = \frac{A \cdot B_{\delta} \cdot \cos\zeta}{\sqrt{2}}, \quad (4)$$

where the A is the sinusoidal linear current density RMS values, B_{δ} is the peak air-gap flux density and ζ is the phase shift between them. For asynchronous machines the value for $\cos\zeta$ is 0.8. The acceptable linear current density depends on material and cooling solution used, e.g., for totally enclosed asynchronous machines reasonable values for A are 30-65 kA/m. With this type of machine the air-gap flux density value B_{δ} to 0.7-0.9 T depending on the air-gap length [16]. For the preliminary design, the tangential stress gives a good starting point for the design, as the required torque can be created on a small surface or a large surface and e.g., the problem with a small surface is the cooling, as the losses need to be removed from the electric machine core. The produced torque is then,

$$T = \sigma_{\text{Ftan}} \cdot r_{\text{r}} \cdot S_{\text{r}}, \quad (5)$$

where r_r is the rotor radius and S_{r} is the surface area of the rotor [16]. The surface velocity can be related to the EM topology, e.g., a solid rotor can achieve a higher value than laminated structure and therefore used as a base to calculate the d_{em} with equation (1), therefore the length of the active part, l_{em} can be calculated from S_{r}.

The AMB designs are often required to maximize force capacity and ensure dynamical performance on limited space, to yield compact designs. In this study, the design of AMB itself is considered out of scope but the dimensions of rotor sections dedicated to the AMB are calculated analytically by the specific load capacity. The higher the specific load capacity, the more demanding the materials needed are [24]. The levitation force generated by the AMB can be given as

$$F_{\text{AMB}} = \sigma_{\text{AMB}} \cdot l_{\text{AMB}} \cdot d_{\text{AMB}}, \quad (6)$$

where σ_{AMB} is the achievable pressure, l_{AMB} and d_{AMB} are the bearing length and diameter, respectively. To obtain the required bearing load, F_{AMB}, the F_{static} including a safety factor needs to be achieved. As per [25], this force should be sufficient enough to prevent contact between the rotor and the stationary components in all expected conditions. For the given design, a factor related to the static load is used to account for dynamic loading

$$F_{\text{static}} = m \cdot g \cdot k_{\text{sf}}, \quad (7)$$

where k_{sf} is the factor of safety for dynamic loading, m is the mass of the rotor and g is the acceleration due to gravity. It should be noted that the factor should be defined based on the application case. Using equations (6) and (7), d_{AMB} can then be calculated.

Considering design constraints for AMBs, external disturbances, unbalance, and loads define the needed force capacity. For IMs with small airgaps, the unbalance magnetic

pull (UMP) can have a significant effect on the AMB–rotor control system performance. The effect depends on relative eccentricity of the IM rotor and centers of AMB planes with respect to the airgap. The static eccentricity is seen as a destabilizing negative stiffness by the AMB–rotor system. Generally, cases where motor rotor eccentricity can be greater than 5% of the motor nominal airgap, should be analyzed for additional force capacity. For example, for a 1 MW slitted solid rotor IM and 10% rotor airgap static eccentricity, the UMP forces reach about 400 N (250 N) at no load (full load) conditions according to FEM. Additionally, about 50 N (30 N) pole number and slot number harmonics are present. The AMBs are sized to fulfill force capacity and bandwidth requirements. For most applications and horizontal rotors, low frequency force capacity is the most important. Based on industrial AMB-rotor systems presented in the literature (and comfortable control lift off and low frequency operation) a nominal overall force capacity of radial AMBs is selected as 5-7 times the gravity force, e.g., 6.24 in [26]. For vertical rotors this force capacity to rotor weight ratio can be lower, e.g., 1.13 in [27]. The feasible ratio value depends on uncertainties in process modelling, force nonlinearities, actuator and sensor noise and delays, machine assembly, and how they affect robust stability of the closed loop system. The laminated AMB force bandwidth f_{BW} (Hz) is the function of DC link voltage u_{DC}, AMB inductance L_{AMB}, and the maximum current $i_{\max}$

$$f_{\mathrm{BW}} = \frac{\ln(9) u_{\mathrm{DC}}}{2\pi L_{\mathrm{AMB}} i_{\max}}, L_{\mathrm{AMB}} = \frac{\mu_0 N^2 S_{\mathrm{air}}}{\frac{l_{\mathrm{Fe}}}{\mu \mathrm{Fe}} + 2(l_0 - x)} \quad (8)$$

where S_{air}, μ_0, μ_{Fe}, and x are effective pole area, relative permeability of air, relative permeability of iron, and displacement from nominal airgap l_0. l_{Fe} is the equivalent flux path length in the actuator iron. The required bandwidth depends on the unbalance and process dynamic loads.

For the remaining sections of the rotor shaft (e.g., rotor end sections, general steps or shoulders), the initial dimensions are more flexibly assigned. In terms of diameter, the end shafts need to be stiff enough to accommodate the impellers. The auxiliary bearings also effect the end shaft dimensions. Usually angular contact ball bearings (ACBB) are used as auxiliary bearing because of their ability to carry high axial and radial loads in touchdown events [28]. The bearing should be able to rotate at the same speed as the operational speed of the rotor, which becomes a limiting factor for the bearing bore diameter and consecutively the shaft diameter of that section, d_{end}.

For the length of the section l_{end}, the section of the rotor typically accommodates one or two single row ACBB, along with an impeller and an axial AMB disc on either end in for e.g., compressor applications. Therefore, twice the width of the selected ACBB with some additional length for ease of fitting is desirable along with the length to accommodate a disc or impeller. Provided dimensions of all other sections have been fixed, the length of the end shafts can be based on the rotordynamics. For example, if the aim is to design a subcritical rotor, the length of the end shaft, l_{end} can be varied as long as the 1st critical speed of the rotor is 20% above the operational speed of the rotor.

For the full rotor of AMB supported rotor, the nodal locations of vibration modes are of interest as those have an effect on the control design. When nodal locations are in the sensor location or actuator location, the mode can not be sensed or controlled with the actuator. [6]. Therefore the nodal locations of vibration modes should be considered and their distance from sensors and actuators studied. In the study a 5% of the rotor total length is considered to be a reasonable amount to have authority on the specific vibration mode.

From the above boundary conditions, a baseline model is formed, which can be optimized based on the rotordynamics. The maximum diameter (active part) is obtained as a result of mechanical stresses, the minimum length of the active part is determined by the tangential stresses of EM, which are related to the cooling capacity (the higher the tangential stresses are, the more effective the cooling is required to be) [16]. Magnetic bearings have a calculated minimum area for the desired load capacity where the radius can be set in relation to the diameter of the active part. Diameters of the rotor ends can be optimized from the dimensioning of the magnetic bearing downwards; the total length being formed by adding the unchanged structures (reservations) defined at the beginning of the design. Auxiliary bearings for example, have a limited capacity for high-speed applications and therefore limit the maximum diameter of rotor ends.

D. Optimization approach description

After creating a baseline model, it is important to critically assess the behavior e.g., by testing few configurations to confirm that the behavior is correct. In addition, for industrial machines the manufacturability and standards requirements should be considered, e.g. API 617 for compressor application. This step requires acute professionalism from the designer on a broader front due to the important detail requirements. This therefore includes some of the most challenging parts of the process.

The baseline model and its parameter exploration (optimization) requires a formulation of the problem to be solved that includes the design variables that are to be changed, the objectives or targets to be maximized or minimized, and the constraints that need to be satisfied. This step requires detailed knowledge of the engineering design and numerical optimization methods as well.

The design variables are the parameters to be optimized, i.e., the parameter relations to other parameters. These variables are independent and subjected to specific boundary conditions. The parameters used in the model can be selected as design variables, e.g., impeller mass, bearing load capacity and shaft dimensions.

The constraint functions are then introduced to ensure that the design is practically feasible. In terms of a slitted rotor configuration in an IM design, the mechanical and electromagnetic tangential stresses can be considered to be an important inequality constraint such that they should be

below the allowed value, e.g., material yield strength or the maximum temperature. Another significant equality constraint with AMBs is the ratio of the bearing load and the force generated by the bearing limited by the attainable specific load capacity with electromagnets.The constant load which a bearing should be capable of achieving includes static and dynamic loads which it will encounter during operation. The dynamical loads are case dependent and are typically an integer multiplication of static load.

Lastly, the objective functions are set for the optimization problem. For the purpose of this study, the objective function is comprised of both rated outputs of the machine as well as the criteria related to rotordynamic behaviour. Each objective function should be defined such that the scalar output of the function is minimized or maximized as a result of the optimization. In terms of desired output, the functions that should be maximized are power or torque, surface velocity while the function that should be minimized is the rotor mass. In terms of rotordynamics, the critical speeds should be maximized to achieve a high rotation speed, and the nodal points of the mode closest to the operational speed should be at maximum distance from the actuators and sensor locations to be able to detect the modes and have authority to control the modes.

Even when a design is seemingly optimal, practical judgement is often required to evaluate the feasibility of the design. In addition to interpreting the optimal design, a post-optimal study also provides insight related to design trends through a parametric study of design variables and their effect on the objectives and constraints.

Figure 3 summarizes the optimization problem formulation from the mechanical design perspective including mechanical design, stresses and rotordynamics, while considering the most important electromagnetic and thermal boundary conditions. Optimization benefits from the method's speed. Based on the baseline model, different design configurations can be calculated using the dimensions of different sub-areas as vectors. The result is a design matrix from which the effects can be analyzed manually or with automated methods between different configurations, for example as shown in Ghalamchi et al. [29]. The baseline model can be changed towards an optimal direction and the analysis performed again within a denser range of values. This allows the creation of a DS that shows the impact of changes in different areas.

III. General case of slitted rotor in induction machine

Typically, the objective of an optimization procedure is to improve the motor efficiency, remaining useful life of a motor or bearings, or similar large scale parameters. However, the exact application and the motor topology sets the initial requirement of the machine [16]. To that end, the test case in this study is a generalized rotor with a slitted active part in IM, and four sections on either side to accommodate, radial bearings, an axial bearing, sensors and an impeller. The idea of using a general test case is that the dimensions can be easily modified based on the power and speed requirements while accounting for the multidisciplinary aspects.

A. Rotordynamics model

For the purpose of studying the dynamical behavior, a finite element (FE) model of the rotor bearing system is used. Figure 4 shows the FE discretized sketch of the rotor along with the rotor baseline dimensions. The baseline dimensions, mass properties and bearing properties are the input for the FE model which then provides the total mass and natural frequencies of the system. The critical speeds of the rotor bearing system are assessed with linearized AMB position stiffness of $2.5{\cdot}10^6$ N/m [30].

B. Baseline for test case

Figure 4 shows the general geometric parameters which are to be derived from the output first and then their sensitivity to output parameters is studied. The geometrical dimensions of interests are the active part of the rotor (l_{em}, d_{em}), the bearing sections (l_{amb}, d_{amb}), rotor ends (l_{end}, d_{end}), and other general sections (l_{s1}, d_{s1}, l_{s2}, d_{s2}), where d stands for the diameter and l for length. The sensor and end ring are assumed to have fixed lengths (l_{sens}, l_{cu}) and diameters (d_{amb}, d_{em}) same as their adjacent sections respectively. Selecting wanted rotation speed (ω) and power (P) for a slitted IM EM, the dimensions are inversely calculated using simple analytical equations (Eqs 1-8) and FE-model for rotordynamics. This way, the dimensions are directly correlated to the desired output and can be used as initial baseline values to study the varied parameters' sensitivity to the outputs. In the test case, outputs are related to rotordynamics first backward and forward whirling frequencies (1st BW, 1st FW), rotor total mass (Mass), torque (T), power (P), electric machine surface velocity ($v_{\text{s,max}}$), static and nominal bearing load capacity (F_{static} & F_{AMB}). Here, the static is load by gravity and nominal load capacity is multiplied by a factor of 4, tangential stress (EM stress), mechanical stress from the centrifugal force in the EM active part, and AMB load capacity.

While the baseline dimensions are primarily calculated analytically from the requirements (rated power and speed), there are a few other assumptions based on the slitted EM configuration. The rotor slit configuration is considered with a slit depth to outer radius ratio of 0.5 and the nominal stress at the tooth is calculated with a stress factor of 4 [22]. Slit thickness was selected to 2.5 mm, which can be manufactured with a DIN 138 compliance groove milling blade. The selected number of rotor axial slits is 38 [31]. The section diameter at AMB location is assumed for the shaft as being 0.5-0.6 times and for lamination outer diameter as 0.7 times the active part diameter to accommodate, the AMB stator and EM end windings and e.g. allow copper end ring installation to enhance the EM performance. The length of the rotor ends are also an important parameter for optimization based on natural frequencies and techniques used for attaching impellers, but for initialization, the end lengths are considered as being half of active part length. Axial disk outer diameter is assumed

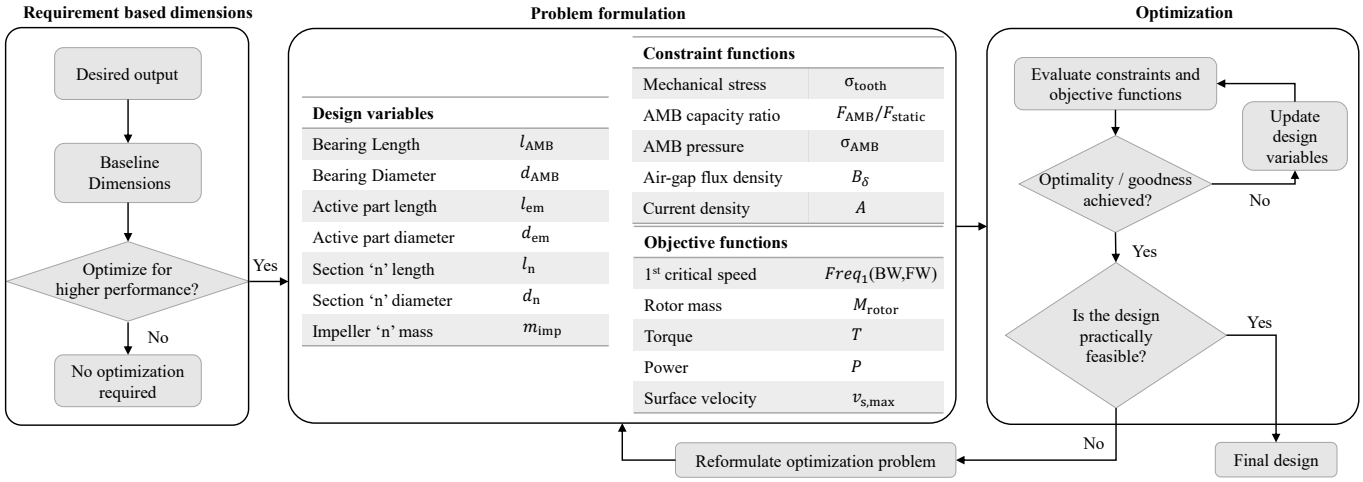

Fig. 3. Design Space procedure

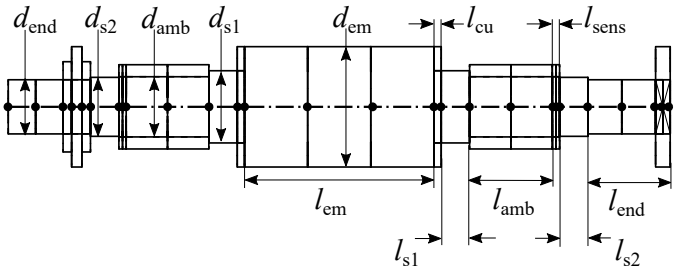

Fig. 4. The rotor structure of the case study with geometrical dimensions of interest. The figure also shown the FE discretization used in the simulation model.

to be the same as EM outer diameter to maximize the load capacity, and in addition to length one third of shaft end length, l_{end}. For the auxiliary bearing, the maximum attainable speed of the roller along the pitch diameter is approximately 100 m/s with 719 series bearings and therefore limiting the maximum bore diameter [32].

IV. Results

In this section, a baseline design is calculated for a selected case from literature [2], [33], [34] by using the equations (1-7), creating a FE-model and using the literature values shown in Section II-B. The case is a 350 kW, 15000 rpm and subcritical operating IM with slitted solid rotor configuration, supported by two AMBs. Once the baseline dimensions are calculated, they are compared with the dimensions from the actual machine.

A. Verification of a baseline design with literature case

The design requirements of literature motor, as described in [2], [33], [34], were used as inputs for the baseline calculation. Therefore, for the same requirements, the baseline dimensions can be compared with those from the literature. As described in [33], the literature rotor is already optimised for electrical and mechanical performance and thus serves as a benchmark for the calculation tool's performance and to evaluate the effectiveness of previous optimization.

Table I shows that baseline dimensions d_{end} and d_{S2} are increasing by 19.1% and 0.9%, respectively in diameter while other dimensions were decreasing (1-39%). It should be noted that the end shaft diameters are the maximum possible diameter so it can be reduced if required to make the rotor lighter. On the contrary, since the first bending mode is considerably higher for the rotor compared to the operational speed, the rotor should be able to work with larger impellers, which can be structurally supported by the end shafts with larger diameter.

Figure 5 shows the cross section of case study rotor overlaid with rotor geometry shown in literature [33]. The results are obtained with average current flux density from literature values, A is 47.5 kA/m and for airgap flux density, B_δ is 0.8. For AMBs 300 kPa specific load capacity is used. Using the desired output values (shown in Table I), the dimensions of the rotor sections are inversely calculated. If these dimensions are different from the ones used in the existing design, they will be used as new baseline values which would lead to an initial direct optimization, i.e. revealing the changes in the design which yields better overall performance. From the design table, the configuration corresponding to the case study rotor dimensions is picked out to verify the model with real world application.

Fig. 5. Cross section of case study rotor (grey) and rotor geometry using baseline dimensions (orange)

Although some direct optimization in rotor dimensions and first bending mode is observed in the verification stage,

TABLE I
BASELINE DIMENSIONS VERSUS LITERATURE CASE WITH SAME DESIGN REQUIREMENTS

Parameters	Ref. [33]	Baseline	Deviation (%)
Rotordynamic Parameters			
Rotor mass(with impeller) (kg)	102.5	75.3	36.1
Impeller mass (kg)	2.86	2.86	-
First critical speed- BW (Hz)	480	616	22.1
First critical speed- FW (Hz)	638	690	7.5
1st mode nodal location from sensors 1, 2 (mm)	175.2, 47.8	73.7, 30.1	-
1st mode nodal location from actuators 1, 2 (mm)	115.2, 107.4	15.4, 28.9	-
Active area from slit stress (Mech)			
Active part diameter(mm), d_{em}	195	164.8	18.3
Slit max depth (mm)	-	41.0	
Slit depth ratio	-	0.5	
Nominal stress in tooth (MPa)	-	88.7	
Number of slit	-	38.0	
Slit width (mm)	-	2.5	
Surface velocity (m/s)	-	130.4	
Active area from Tangential Stress (EM)			
Tangential stress from EM Force (Pa)	-	21496.1	
Active part length (mm) l_{em}	330	243.0	35.8
AMB section			
Diameter of AMB (mm), d_{amb}	84	82.4	1.9
Length of AMB (mm), l_{amb}	110	106.7	3.1
Rotor end shaft and back up bearing section			
Diameter (mm), d_{end}	60	74.2	19.1
Length (mm), l_{end}	120	106.1	13.1
General sections			
Section 1 Diameter (mm), d_{S1}	106	98.9	7.2
Section 1 Length (mm), l_{S1}	46	36.5	26.0
Section 2 Diameter (mm), d_{S2}	80	80.7	0.9
Section 2 Length (mm), l_{S2}	43	36.5	17.8
Fixed dimensions			
Sensor length (mm), l_{sens}	10	10	-
End ring length (mm), l_{cu}	10	10	-

the baseline is an initial starting point for the design space exploration, and therefore, should be considered as suggested dimensions. Once the baseline is ready, further possibilities can be explored.

B. Design space exploration

For exploring different design possibilities, the optimization approach suggested in section II-D usually provides a range of values for multiple objective functions rather than a single 'perfect' combination. The range of outputs provides design trends and correlations between different parameters while the objective functions compensate for each another. Based on the application requirement, the designer can settle for a particular combination of objective functions, and thereby select a corresponding set of design variables.

For simplification, a manual iteration process is carried out in this study instead of a full optimization to generate a range of objective functions based on different combinations of design variables. Each design variable is varied by a unit from the baseline design (Table I) and the difference in outputs are studied, i.e., the sensitivity of each design variable to output. Table II shows the per unit (PU) change effect on output parameters in percentages.

V. DISCUSSION

The baseline model based on the values which can be referenced yielded to a very similar structure which was reported in a case study found in literature (see Section IV-A). This suggests that values based on earlier studies give a good approximation for the given EM topology. The baseline used as the starting point for design space exploration, showed clearly the effect of different sections of the baseline machine and their influence on other parameters. It should be noted that slit-IM configuration was used in the study, and for other IM topologies, such as full squirrel cage, the stress calculations with analytical equations are more complicated.

TABLE II
DESIGN EXPLORATION FROM BASELINE MODEL WITH PER UNIT (PU) ADDITION TO DIMENSION

parameter varied (+per unit)	Effect (%)						
	1st BW	1st FW	Mass	T/P	$v_{\text{s,max}}$	F_{static}	F_{AMB}
l_{end}	-0.50	-0.55	0.13	0.00	0.00	0.13	0.00
l_{s2}	-0.51	-0.58	0.11	0.00	0.00	0.11	0.00
l_{AMB}	-0.50	-0.54	0.22	0.00	0.00	0.22	0.94
l_{s1}	-0.41	-0.45	0.16	0.00	0.00	0.16	0.00
l_{EM}	-0.08	-0.10	0.18	0.41	0.00	0.18	0.00
d_{end}	-0.29	-0.36	0.22	0.00	0.00	0.22	0.00
d_{s2}	0.10	0.09	0.10	0.00	0.00	0.10	0.00
d_{AMB}	0.89	1.00	0.63	0.00	0.00	0.63	1.21
d_{s1}	0.40	0.43	0.12	0.00	0.00	0.12	0.00
d_{EM}	-0.01	0.02	0.67	1.24	0.61	0.67	0.00
m_{imp}	-3.67	-4.31	1.25	0.00	0.00	1.25	0.00

The design exploration chart in Table II shows how changing the dimensions and impeller mass affected the overall outputs. While the electromagnetic and mechanical stresses remain unchanged for unit deviation of dimensions in millimeters/kilograms, parameters such as torque power are linearly correlated with active part dimensions, and therefore can be seen increasing linearly with increases in active part diameter. AMB related parameters such as static load capacity (F_{static}) behaves in a similar manner as the rotor mass, while the nominal load capacity is only affected linearly by the AMB related dimensions.

The most significant effects can be seen on the rotordynamics, where the 1st forward (FW) and backward (BW) whirling modes defining subcritical operation, are affected by the design variables. Increasing the length of the rotor ends and the AMB sections, reduce the 1st forward and backward critical speeds the most, followed by the active part length. In comparison to the other section, the rotor ends contribute the least to the stiffness of the system and when further elongated, the overall stiffness further reduces, thereby decreasing the 1st bending mode critical speeds. In terms of diameter, increasing the diameter in the bulk section of the rotor such as the AMB section or the active part increases the critical speeds, whereas increasing diameter in end sections lowers the 1st bending mode critical speeds. The added diameter and therefore mass in the end sections acts similar to the overhang mass.

VI. CONCLUSIONS

In the study Design Space method (DSM) for high-power, a high-speed IM machine with a slitted rotor is developed. With power and speed requirements together with general constraints, which can be found in literature, baseline design is generated by DSM. By having constraints on the EM tangential stress, mechanical stress, AMB's specific load capacity, and slitted rotor analytical equations the full rotor geometry was generated. The baseline design was then compared to

a literature case study and the differences in design were assessed. The DSM was able to yield a design similar to the literature case. This proves the ability of the proposed method to generate design spaces, which enables different design alternatives, parameter sensitivity or more radical design iterations. For a multidisciplinary design problem, the method enables the opportunity to create a blank design, which can be optimized in the detail design. This is important in high-power and high-speed machines, where the design times are lengthy, and therefore prevents wider utilization due to the high design costs. The baseline model was further studied by the parameter exploration and identified the effect of changing parameters, suggesting for designer insight into specific design selections. The method is applicable for other high-speed machines and based on the defined boundary conditions its suitability can be benchmarked. For further studies, the comparison of the method to other cases and e.g., laminated structures is of interest.

ACKNOWLEDGEMENT

Funding: This work was supported by the Business Finland Brain-project [decision number 1119/31/2018].

REFERENCES

[1] E. Kurvinen. Design and simulation of high-speed rotating electrical machinery. *Acta Universitatis Lappeenrantaensis*, 2016.

[2] A. Smirnov, N. Uzhegov, T. Sillanpää, J. Pyrhönen, and O. Pyrhönen. High-speed electrical machine with active magnetic bearing system optimization. *IEEE Transactions on Industrial Electronics*, 64(12):9876–9885, 2017.

[3] H. Kim, E. Sikanen, J. Nerg, T. Sillanpää, and J. T. Sopanen. Unbalanced magnetic pull effects on rotordynamics of a high-speed induction generator supported by active magnetic bearings – analysis and experimental verification. *IEEE Access*, 8:212361–212370, 2020.

[4] P. Cui, S. Li, Q. Wang, Q. Gao, J. Cui, and H. Zhang. Harmonic current suppression of an amb rotor system at variable rotation speed based on multiple phase-shift notch filters. *IEEE Transactions on Industrial Electronics*, 63(11):6962–6969, 2016.

[5] S. Zheng, Q. Chen, and H. Ren. Active balancing control of amb-rotor systems using a phase-shift notch filter connected in parallel mode. *IEEE Transactions on Industrial Electronics*, 63(6):3777–3785, 2016.

[6] E. H. Maslen and G. Schweitzer. *Magnetic bearings: theory, design, and application to rotating machinery*. Springer, 2009.

[7] J. Driesen and R. Belmans. Specific problems of high-speed electrical drives. In *9th International Fluid Power Conference*, 2005.

[8] J. A. Swanke, D. Bobba, T. M. Jahns, and B. Sarlioglu. Design of high-speed permanent magnet machine for aerospace propulsion. In *2019 AIAA/IEEE Electric Aircraft Technologies Symposium (EATS)*, pages 1–12, 2019.

[9] N. Uzhegov, E. Kurvinen, J. Nerg, J. Pyrhönen, J. T. Sopanen, and S. Shirinskii. Multidisciplinary design process of a 6-slot 2-pole high-speed permanent-magnet synchronous machine. *IEEE Transactions on Industrial Electronics*, 63(2):784–795, 2016.

[10] P. Lindh, P. Immonen, C. Di, M. Degano, and J. Pyrhönen. Solid-rotor material selection for squirrel-cage high-speed solid-rotor induction machine. In *IECON 2019 - 45th Annual Conference of the IEEE Industrial Electronics Society*, volume 1, pages 1357–1361, 2019.

[11] J. Pyrhönen, J. Nerg, A. Mikkola, J. Sopanen, and T. Aho. Electromagnetic and mechanical design aspects of a high-speed solid-rotor induction machine with no separate copper electric circuit in the megawatt range. *Electrical engineering*, 91(1):35–49, 2009.

[12] A. Arkkio, T. Jokinen, and E. Lantto. Induction and permanent-magnet synchronous machines for high-speed applications. In *2005 International Conference on Electrical Machines and Systems*, volume 2, pages 871–876 Vol. 2, 2005.

[13] Z. Kolondzovski, A. Arkkio, J. Larjola, and P. Sallinen. Power limits of high-speed permanent-magnet electrical machines for compressor applications. *IEEE Transactions on Energy Conversion*, 26(1):73–82, 2011.

[14] C.J.G Ranft. *Mechanical design and manufacturing of a high speed induction machine rotor*. PhD thesis, North-West University, 2010.

[15] F. Cheng, H. Xu, and S. Xue. Study on the design method of high speed permanent magnet synchronous machine. In *2011 International Conference on Electrical Machines and Systems*, pages 1–6, 2011.

[16] J. Pyrhönen, T. Jokinen, and V. Hrabovcova. *Design of rotating electrical machines*. John Wiley & Sons, 2013.

[17] W.J. Chen. *Introduction to dynamics of rotor-bearing systems*. Trafford publishing, 2007.

[18] R. R. Moghaddam. High speed operation of electrical machines, a review on technology, benefits and challenges. In *2014 IEEE Energy Conversion Congress and Exposition (ECCE)*, pages 5539–5546, 2014.

[19] A. Tonoli, A. Bonfitto, M. Silvagni, L.D. Suarez, and F. Beltran-Carbajal. Rotors on active magnetic bearings: Modeling and control techniques. In *Advances in Vibration Engineering and Structural Dynamics*, pages 1–3. InTech, 2012.

[20] R. P. Jastrzebski and O. Pyrhönen. Design of high flux density active magnetic bearings for high-speed multi megawatt motor. In *2018 20th European Conference on Power Electronics and Applications (EPE'18 ECCE Europe)*, pages P.1–P.9, 2018.

[21] A. Borisavljevic, H. Polinder, and J. A. Ferreira. On the speed limits of permanent-magnet machines. *IEEE Transactions on Industrial Electronics*, 57(1):220–227, 2010.

[22] T. Aho, J. Nerg, J. Sopanen, J. Huppunen, and J. Pyrhönen. Analyzing the effect of the rotor slit depth on the electric and mechanical performance of a solid-rotor induction motor. *International Review of Electrical Engineering (IREE)*, 1(4):516–525, 2006.

[23] A. Borisavljevic. *Limits, modeling and design of high-speed permanent magnet machines*. Springer Science & Business Media, 2012.

[24] E. Swanson, A. Masala, and L. Hawkins. New active magnetic bearing requirements for compressors in api 617 eighth edition. In *Proceedings of the 43rd Turbomachinery Symposium*. Texas A&M University. Turbomachinery Laboratories, 2014.

[25] API 617 Standard. Axial and centrifugal compressors and expander-compressors. 2014.

[26] N. Takahashi and S. Kaneko. Thermal instability in a magnetically levitated doubly overhung rotor. *Journal of Sound and Vibration*, 332(5):1188–1203, 2013.

[27] A. Grönman, J Nerg, E. Sikanen, T. Sillanpää, N. Nevaranta, E. Scherman, A. Uusitalo, N. Uzhegov, A. Smirnov, J. Honkatukia, P. Sallinen, R. P. Jastrzebski, J. Heikkinen, J. Backman, J. Pyrhönen, O. Pyrhönen, J. Sopanen, and T. Turunen-Saaresti. Design and verification of a hermetic high-speed turbogenerator concept for biomass and waste heat recovery applications. *Energy Conversion and Management*, 225(September):113427, 2020.

[28] N. Neisi, J. Heikkinen, T. Sillanpää, T. Hartikainen, and J. Sopanen. Performance evaluation of touchdown bearing using model-based approach. *Nonlinear Dynamics*, 101(1):211–232, 2020.

[29] B. Ghalamchi, A. Kłodowski, J. Sopanen, and A. Mikkola. Genetic optimization of geometrical parameters of high speed rotor. In *International Design Engineering Technical Conferences and Computers and Information in Engineering Conference*, volume 57181, page V008T13A016. American Society of Mechanical Engineers, 2015.

[30] J. Vuojolainen, N. Nevaranta, R. P. Jastrzebski, and O. Pyrhönen. Comparison of Excitation Signals in Active Magnetic Bearing System Identification. *Modeling, Identification and Control*, 38(3):123–133, 2017.

[31] J. Huppunen. *High-speed solid-rotor induction machine–electromagnetic calculation and design*. Lappeenranta University of Technology, 2004.

[32] SKF. Super-precision angular contact ball bearings: High-capacity, 2021.

[33] J. E. Heikkinen, A. Smirnov, V. Hakonen, and J. Sopanen. Virtual testing of amb supported rotor-system. In *Proceedings of the 14th IFToMM World Congress*, pages 465–471, 2015.

[34] V. Hakonen. Virtual Testing of Active Magnetic Bearing Systems based on Design Guidelines given by the Standards. Master's thesis, Lappeenranta University of Technology, Finland, 2014.